The Astrophysical Journal, 803:101 (7pp), 2015 April 20 doi:10.1088/0004-637X/803/2/101

ARE MODELS FOR CORE-COLLAPSE SUPERNOVA PROGENITORS CONSISTENT WITH THE PROPERTIES OF SUPERNOVA REMNANTS?

Daniel J. Patnaude[1], Shiu-Hang Lee[2], Patrick O. Slane[1], Carles Badenes[3], Alexander Heger[4], Donald C. Ellison[5], and Shigehiro Nagataki[6]
[1] Smithsonian Astrophysical Observatory, Cambridge, MA 02138, USA; dpatnaude@cfa.harvard.edu, pslane@cfa.harvard.edu
[2] Institute of Space and Astronautical Science, Japan Aerospace Exploration Agency, 3-1-1 Yoshinodai, Chuo-ku, Sagamihara, Kanagawa 252-5210, Japan; slee@astro.isas.jaxa.jp
[3] Department of Physics and Astronomy and Pittsburgh Particle Physics, Astrophysics and Cosmology Center (PITT PACC), University of Pittsburgh, 3941 O'Hara Street, Pittsburgh, PA 15260, USA; badenes@pitt.edu
[4] Monash Center for Astrophysics, School of Mathematical Sciences, Building 28, Monash University, Vic 3800, Australia; alexander.heger@monash.edu
[5] Physics Department, North Carolina State University, Box 8202, Raleigh, NC 27695, USA; don_ellison@ncsu.edu
[6] RIKEN, Astrophysical Big Bang Laboratory, 2-1 Hirosawa, Wako, Saitama 351-0198, Japan; shigehiro.nagataki@riken.jp
Received 2014 December 23; accepted 2015 February 15; published 2015 April 22

ABSTRACT

The recent discovery that the Fe–K line luminosities and energy centroids observed in nearby supernova remnants are a strong discriminant of both progenitor type and circumstellar environment has implications for our understanding of supernova progenitor evolution. Using models for the chemical composition of core-collapse supernova (CCSN) ejecta, we model the dynamics and thermal X-ray emission from shocked ejecta and circumstellar material, modeled as an r^{-2} wind, to ages of 3000 yr. We compare the X-ray spectra expected from these models to observations made with the *Suzaku* satellite. We also model the dynamics and X-ray emission from Type Ia progenitor models. We find a clear distinction in Fe–K line energy centroid between core-collapse and Type Ia models. The CCSN models predict higher Fe–K line centroid energies than the Type Ia models, in agreement with observations. We argue that the higher line centroids are a consequence of the increased densities found in the circumstellar environment created by the expansion of the slow-moving wind from the massive progenitors.

Key words: ISM: abundances – ISM: supernova remnants – stars: mass-loss – supernovae: general – X-rays: ISM

1. INTRODUCTION

Supernovae, both thermonuclear (Ia) and core-collapse (CC), represent the endpoints in the stellar evolution of either Chandrasekhar white dwarfs or massive stars with zero age main sequence masses $>8\,M_{\odot}$. Core-collapse supernovae (CCSNe) exhibit a wide diversity of properties. Classifications are based on spectra and light curves, and not necessarily on a physical mechanism (Filippenko 1997). Types I and II are determined by the presence (II) or absence (I) of H lines in the spectrum. Type I CCSNe include Type Ib/c, Ibn, and Ic-BL. The progenitors of these supernovae are thought to be either massive He stars or some subset of Wolf–Rayet (WR; see Gal-Yam et al. 2007, for a broad classification). Type II SNe include the subtypes IIP (e.g., SN 1999em; Smartt et al. 2002) IIL (e.g., SN 1979C; Fesen & Matonick 1993), II-pec (e.g., SN 1987A; Chevalier & Emmering 1989), IIn (e.g., SN 1995N; Fransson et al. 2002), IIb (e.g., SN 1993J; Fransson et al. 1996), and possibly some superluminous supernovae that exhibit evidence for a strong circumstellar interaction, such as SN 2006tf (Smith et al. 2008).

Unlike Type I CCSNe, the progenitors of Type II supernovae are likely red or yellow supergiants (R/YSG), or in the case of IIn, luminous blue variables (LBVs; Gal-Yam et al. 2007). In at least a few cases, progenitors have been identified in pre-explosion images (Smartt 2009). In both Type I and II CCSNe, the progenitor mass-loss rate can vary between 10^{-6} and $10^{-4}\,M_{\odot}\ \mathrm{yr}^{-1}$ (and for IIns and SLSNe, 0.1–10 $M_{\odot}\ \mathrm{yr}^{-1}$, presumably as eruptive mass-loss), but the wind velocity (v_w) between the RSG or WR progenitor can differ by as much as two orders of magnitude ($v_w = 10$–$20\ \mathrm{km\ s}^{-1}$ in a RSG, and $\sim$1000 $\mathrm{km\ s}^{-1}$ in a WR star; Crowther 2007; Smith 2014). For steady, isotropic mass-loss, the circumstellar medium (CSM) density is proportional to $\dot{M}/v_w$. Thus high mass-loss rates coupled with slow wind velocities can lead to a substantial amount of mass close to the supernova progenitor. This would be in contrast to the large, evacuated cavities expected around WR progenitors, due to their large mechanical wind luminosities (see Koo & McKee 1992).

While typing supernovae based on their optical spectra is well established (Filippenko 1997), connecting supernovae types to supernova remnants (SNRs) remains difficult. In the case of Type Ia supernovae, their remnants can frequently be readily identified by the iron content observed in the X-ray spectrum (Hughes et al. 1995; Badenes et al. 2006, 2008; Patnaude et al. 2012). Given the broad diversity of CCSN types, connecting remnants to supernovae (and to supernova models) is a challenge. However, examples exist where supernovae have been linked to SNRs, or SNRs have been directly typed. For instance, light echo analysis allows for direct typing of some SNRs such as Cas A (Fransson et al. 1996; Krause et al. 2008; Rest et al. 2008), and Milisavljevic et al. (2012) recently showed that the [O III] line shape in SN 1993J was remarkably similar to that of Cas A. Finally, similarities in X-ray spectra provide evidence that SN 1996cr may be a Type II pec, similar to SN 1987A (Bauer et al. 2008). However, beyond these examples, connections between SNe and SNRs remain sparse, particularly for the class of CCSNe (Hughes et al. 1995).

Recently, Yamaguchi et al. (2014) presented a method of typing SNRs based on the Fe–Kα line centroid and luminosity. Since Fe is produced in the center of the progenitor during the explosion, heating of Fe can be delayed, resulting in an

Table 1
Model Parameters

Ejecta Model	E_{SN} 10^{51} erg	M_{ej} ($M_\odot$)	n_{amb}[a] (cm^{-3})	v_{wind}[b] (km s^{-1})	$\dot{M}$[b] 10^{-5} $M_\odot$ yr^{-1}	References
DDTa	1.27	1.38	0.1–3.0	⋯	⋯	Badenes et al. (2008)
DDTg	0.85	1.38	0.1–3.0	⋯	⋯	Badenes et al. (2008)
s12D	1.21	8.87	⋯	10–20	1–2	This work
s25D	1.21	12.2	⋯	10–20	1–2	This work
1987A	1.10	14.7	⋯	10–20	1–2	Saio et al. (1988)
1993J	2.00	2.92	⋯	10–20	1–2	Nozawa et al. (2010)

[a] Type Ia models evolve in a constant density environment.
[b] Core-collapse models evolve in a circumstellar environment shaped by isotropic mass-loss.

ionization state lower than He-like (Fe^{24+}) in young and middle-aged SNRs. The ionization state affects the Fe–K line centroid, which can be measured to high precision with current X-ray satellites. Yamaguchi et al. (2014) showed that the Fe–K line centroids for Ia SNRs are generally lower (<6550 eV) than those found in CCSNRs. Additionally, they found that when computing synthetic Fe–K line centroids and luminosities from well tested models for Type Ia ejecta, the models (Badenes et al. 2006, 2008) predicted bulk properties in line with observations (Yamaguchi et al. 2014).

Here we extend the work of Yamaguchi et al. (2014) to address the question of whether models for CCSNe are able to reproduce, in broad terms, the observable bulk properties of CCSNRs. We employ a model that tracks the hydrodynamics and time-dependent ionization of shocked circumstellar material and supernova ejecta, coupled to an emissivity code to compute Fe–K line centroids and luminosity, as a function of supernova ejecta model, age, and circumstellar environment. We compare our models to *Suzaku* observations of Galactic and Magellanic Cloud SNRs, and discuss implications and future directions that this work can take.

2. HYDRODYNAMICAL MODEL

We employ our *CR-hydro-NEI* code which allows us to simultaneously describe the thermal and nonthermal emission at the forward and reverse shocks in young SNRs. *CR-hydro-NEI* is a 1D Lagrangian hydrodynamics code based on VH-1, a multidimensional hydrodynamics code developed by J. Blondin and colleagues (e.g., Blondin & Lufkin 1993). *CR-hydro-NEI* simultaneously models the supernova blastwave dynamics and particle acceleration, including the back reaction of the nonthermal particles on the SNR dynamics. It is capable of modeling the nonthermal particle spectrum as well as the broadband nonthermal and thermal emission from shocked circumstellar material and ejecta. Here, we run the model without considering the effects of diffusive shock acceleration on the dynamics and emitted spectra (i.e., we set the particle injection to the test particle limit). Specific details concerning *CR-hydro-NEI* can be found in Ellison et al. (2007, 2010), Patnaude et al. (2009, 2010), and Lee et al. (2014). Recent modifications to the code allow us to track the evolution of the thermal emission from the shocked ejecta, as well as employ custom ejecta models (Lee et al. 2014).

2.1. Ejecta Models

For this study, we make use of previously available models for the composition of the ejecta in both CC and Type Ia SNe. For the Ia models, we employ the delayed detonation models DDTa and DDTg (Badenes et al. 2003). In these models, a flame propagates as a slow deflagration, with a transition to a detonation induced at some flame density. The transition point sets the amount of ^{56}Ni produced in the explosion. The DDTa model produces ~1 $M_\odot$ of ^{56}Ni, while the less energetic DDTg model produces only ~0.3 $M_\odot$ of ^{56}Ni.

To model the CCSNe, we employ a range of ejecta models from a variety of single star progenitor scenarios. For this paper we have computed new stellar models of 12 $M_\odot$ and 25 $M_\odot$ initial mass, Models s12D and s25D. These models have been computed using the *KEPLER* stellar evolution code (Weaver et al. 1978) and are similar to those in Woosley & Heger (2007; see also Rauscher et al. 2002; Woosley et al. 2002), but use the updated solar abundances from Lodders et al. (2009). For both models, the stellar evolution, including mass-loss, is followed to the point of CC. Model s12D loses approximately 3 $M_\odot$ of material, while Model s25D loses ≈ 8 $M_\odot$ due to stellar winds by the time of CC. Details of the explosion can be found in Rauscher et al. (2002). As a brief summary, a piston is placed at the base of the oxygen burning layer where entropy per baryon rises above $S/k_B = 4$. The piston is first moved inward at about one-fourth of local gravitational acceleration until a radius of 100 km is reached; then it is moved outward at a constant fraction of local acceleration until a radius of 10,000 km is reached. The outward acceleration is adjusted such that an explosion energy of 1.2×10^{51} erg is reached; the estimated explosion energy for SN 1987A is taken as a typical value here. The prescription for mixing in the ejecta can be found in Heger & Woosley (2010), but the default parameters used here have been adjusted such that enough ^{56}Ni is mixed into the envelope to reproduce the light curves of Type II supernovae, in good agreement with hydrodynamic simulations (Joggerst et al. 2009).

We also use a model for CCSN ejecta tailored to SN 1987A (Saio et al. 1988; Hashimoto et al. 1989; Shigeyama & Nomoto 1990). The model comprises a 6 $M_\odot$ Helium star enclosed in a 10 $M_\odot$ hydrogen envelope. Finally, we include a model that has been previously applied to the Type IIb SN 1993J (Shigeyama et al. 1994). The progenitor for this model is an 18 $M_\odot$ main sequence progenitor with a metallicity $Z = 0.02\ Z_\odot$. This progenitor loses ≈15 $M_\odot$ of material prior to core-collapse. Further details of the models are summarized in Table 1.

Though Yamaguchi et al. (2014) have previously shown agreement between Type Ia models and measured Fe–K line centroids and luminosities, we include a subset of Ia models in our sample to validate our results. For reasons discussed below, we do not expect an exact agreement between our Ia results and

those in Yamaguchi et al. (2014), but broad agreement is provided as a consistency check. The CCSN ejecta models are from the evolution of single-star progenitors and thus do not include the effects that binarity have on the progenitor evolution and the circumstellar environment (Sana et al. 2012). We will address the role of binarity on both the progenitor and CSM in a future paper.

2.2. Circumstellar Environments

A key question is the shape of the circumstellar environment around the supernova progenitor. R/YSG expel several solar masses of material over their lifetimes (10^{-6}–10^{-4} $M_{\odot}$ yr^{-1}) with velocities of 10–100 km s^{-1}. WR progenitors expel similar amounts of mass per year, but with wind velocities 100× that of their R/YSG counterparts (e.g., Smith 2014). Additionally, episodic mass-loss may be relevant in the thermal and dynamical evolution of SNe (Pan et al. 2013), resulting in emission that is luminous early on, but decays sharply due to a sudden decrease in the circumstellar density (e.g., Dwarkadas 2011; Dwarkadas & Gruszko 2012). Regardless of details, it is currently accepted that SNe of the Type II variety expel material with velocities ∼10—a few 100 km s^{-1}, while CC of the Ib/c (and variants) have wind velocities ∼1000 km s^{-1} (Smith 2014).

Given the diverse nature of the CSM environment expected around CCSNe progenitors, we chose to take a general approach and consider a range of mass-loss rates and wind velocities appropriate for massive, red supergiant progenitors. We consider progenitor winds with mass-loss rates of $\dot{M}$ = 1–2 × 10^{-5} $M_{\odot}$ yr^{-1}, and wind velocities of v_w = 10–20 km s^{-1}. We do not consider CSM environments shaped by fast winds, e.g., WR and O-type stars, as these winds are expected to result in low density cavities (see, e.g., Dwarkadas 2007). The low density CSM does not lend itself to substantial thermal X-ray emission (e.g., as in SNR RX J1713.7-3946 Ellison et al. 2012), and any shocked CSM has a low temperature due to the long Coulomb heating timescale. For the Ia models, we assume uniform densities with ranges of 0.3–3.0 cm^{-3}, consistent with results inferred from observations of the environments around Ia progenitors (Badenes et al. 2007).

3. MODELING AND RESULTS

We evolve the CCSNe to ages of 3000 yr. Dwarkadas & Chevalier (1998) pointed out that for a Type Ia ejecta model interacting with a constant density ambient medium, the reverse shock propagates to the center of the ejecta when the forward shock has swept up ∼24 × the ejecta mass. For the Ia models considered here, the reverse shock reaches the ejecta center at ages of ∼1000 yr for the densest CSM environments. Thus we only consider the evolution of the Type Ia models to 1000 yr. This differs from Yamaguchi et al. (2014) where they evolve the Ia models to much larger ages, allowing the shock to bounce and re-shock previously shocked ejecta. For both the CC and Ia models, we evolve them over the range of parameters summarized in Table 1, resulting in a grid of models that span a range of circumstellar environments.

The ejecta models include not only the composition as a function of mass coordinate, but also the density and velocity as a function of mass coordinate. For this study, we have mapped the ejecta composition onto approximations of the ejecta structure: the CCSNR models assume ejecta with a constant density core and an n = 9 power law envelope (Truelove & McKee 1999). The Type Ia ejecta are modeled with an exponential ejecta profile (Dwarkadas & Chevalier 1998). Our code produces ionization fractions for both shocked CSM and ejecta as a function of SNR age. We pass these parameters to an emissivity code (Patnaude et al. 2010; Lee et al. 2014) to compute the full SNR spectrum as a function of time. As discussed in Lee et al. (2014), we include thermal and Doppler broadening, though we do not consider their effects on our results here, nor do we consider the individual contributions from shocked CSM versus shocked ejecta as a function of time. Future X-ray observatories such as *Astro-H* may be able to discern between these two components. At chosen time-steps, we used Xspec[7] to synthesize a *Chandra* ACIS-S observation of the SNR. We then fit the 6–7 k eV emission from the simulated observation to a Gaussian with a power law continuum.[8] The results from these simulations, for the grid of Type Ia and CCSNe models lists in Table 1 are shown in Figure 1, where we plot the Fe–K line centroid as a function of luminosity (left panel), as well as the evolution of the Fe–K line luminosity as a function of scaled SNR age (right panel).

4. DISCUSSION

The data in Figure 1 (left) are taken from Yamaguchi et al. (2014). In broad terms, we find results that are consistent to those in Yamaguchi et al. (2014): SNRs typed by their Fe content as Ias are generally consistent with the synthesized X-ray spectra from Ia models. Note that we do not expect an exact match between the results presented in Yamaguchi et al. (2014) and here: our calculations include emission from both shocked ejecta and circumstellar material, while they only consider emission from shocked ejecta; the electron to proton temperature at the shock in their model is assumed to be either 0.01 or 0.03, while we assume mass proportional heating at the shock, followed by Coulomb heating downstream; as discussed in (Patnaude et al. 2010), the collisional ionization and recombination rates used in the ionization balance calculations, as well as the atomic data used in the spectral synthesis likely also differ. However, even with these numerous differences, it is encouraging to find agreement between our Ia results and those presented in Yamaguchi et al. (2014), and gives us confidence that the results for the CC models are insensitive to these differences. The line centroids and luminosities for the CC models are also presented in Figure 1 (left). For those models, we find that the measured Fe–K luminosities and line centroids are consistent with the models, with a few notable exceptions discussed below.

As discussed in Yamaguchi et al. (2014), all Ia SNRs have observed Fe–K line centroids $\lesssim$6550 eV, and the chosen Ia ejecta models also do not produce Fe–K centroids in excess of 6550 eV. Even *Kepler*'s SNR, which is thought to be the result of a luminous Ia in a modified CSM (Chiotellis et al. 2012; Patnaude et al. 2012) still displays bulk properties consistent with a Ia origin.

For the observed CCSNRs, the observed line centroids are broadly consistent with the model predicted centroids and luminosities. In most cases the CC models show Fe line

[7] http://heasarc.gsfc.nasa.gov/xanadu/xspec/

[8] Since we are fitting the simulated spectrum over such a narrow band pass, the continuum, which in reality is thermal in nature and the sum of several shocked components, is well approximated by a power law.

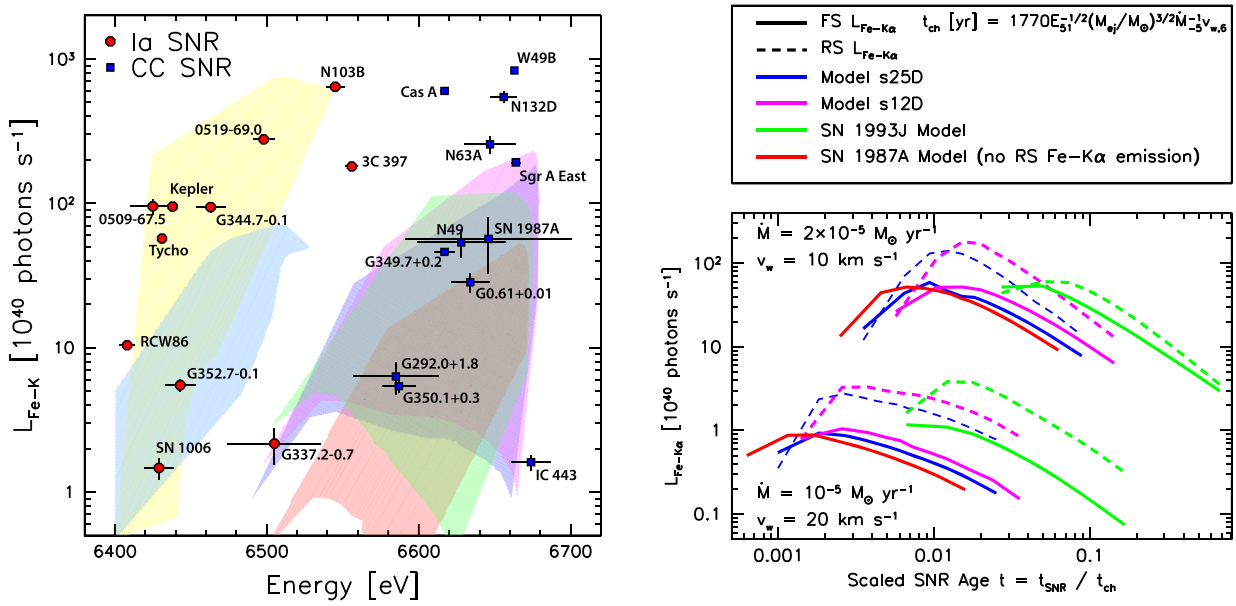

Figure 1. Left: Fe–K line luminosity vs. centroid energy for Galactic and Magallenic Cloud Ia and core-collapse supernova remnants. The transparent shaded regions correspond to the models listed in Table 1 with yellow corresponding to model DDTa, light blue to DDTg, red to 1987A, green to 1993J, magenta to s12D and dark blue to s25D. The data are taken from Table 1 of Yamaguchi et al. (2014). Right: Fe–K luminosity as a function of scaled SNR age. The solid curves are the FS emission, while the dashed curves are for the RS emission. The two sets of curves represent the two sets of models listed in Table 1. The SN 1987A model does not produce any appreciable Fe–K emission from the RS.

centroids that are in excess of 6550 eV. Only in the youngest models ($t_{\rm SNR} \lesssim 200$ yr) do we find Fe line centroids at or below 6550 eV. Yamaguchi et al. (2014) have argued that the higher observed line centroids are likely the result of higher ambient medium density, and our results support this conclusion. For the highest density Ia model, $n_{\rm amb} = 3.0\,{\rm cm}^{-3}$, while for the CC models, even though the density follows a r^{-2} power law, $n_{\rm amb} > 10\,{\rm cm}^{-3}$ at radii in excess of 10^{17} cm, owing to the high density close in to the progenitor. The higher ambient medium density has a two-fold effect: first, the shocked CSM is at a higher temperature and ionization state, since heating $\propto n^2$, and ionization rates are $\propto n$; second, the dense circumstellar environment produces a strong reverse shock which can deposit more energy into the ejecta, resulting in higher overall charge states in the shocked ejecta.

In Figure 1 (right), we plot the time evolution of the Fe–K emission from both the forward and reverse shocks, for the range of mass-loss parameters listed in Table 1. We scale the SNR age to the characteristic SNR age given by Truelove & McKee (1999):

$$t_{\rm ch} = 1770 E_{51}^{-1/2} \left(\frac{M_{\rm ej}}{M_\odot} \right)^{3/2} \dot{M}_{w,5}^{-1} v_{w,6}\ {\rm yr}, \qquad (1)$$

where the ejecta masses and explosion energetics are taken from Table 1. As seen in Figure 1 (right), the emission from swept up circumstellar and shocked ejecta is initially comparable in the s12D, s25D, and SN 1993J models, but the emission from shocked ejecta quickly surpasses that of the shocked circumstellar material by a factor of two or more. Interestingly, and previously pointed out in Lee et al. (2014), there is no appreciable Fe–K emission from shocked ejecta in the SN 1987A models, even at late times (our models do show that the Fe–K emission from shocked ejecta does begin to appear at late times, though remains very weak). The SN 1987A model differs from the other models in two aspects: first, it is a compact blue progenitor, and the densities in the ejecta are higher than in the other models with extended H-rich envelopes, and second, the Fe abundance in the SN 1987A model is ∼two orders of magnitude lower than in the other models—there is not a significant amount of Fe to shock in the ejecta.

We also investigate the relationship between the Fe–K line luminosity and energy centroid and the SNR radius. In Figure 2 we plot the line luminosity as a function of radius for each model (left panels) while in the right panels we plot the line energy centroid as a function of radius. Note that for those models with a high mass-loss rate and low wind velocity, the Fe–K line centroid approaches the collisional ionization equilibrium value in several 100 yr While the measured line centroids as a function of SNR radius do generally agree with the models, the observed line luminosities for as many as half of the sampled remnants are greater than the modeled luminosities by as much as an order of magnitude. We discuss these results in more detail below.

Chevalier (2005) typed several Galactic SNRs based on the properties of the swept up circumstellar material, classifying many as either Type IIb/L or Type IIP. Main sequence progenitors for Type IIP and IIb/L SN span a mass range of 10–25 $M_\odot$, and have slow dense winds resulting in much of the lost mass remaining close to the progenitor. Outside of this is a low density bubble created by the fast wind from the main-sequence phase. Models s12D and s25D represent such RSG progenitors (Heger & Woosley 2010). Model s25D has lost almost 13 $M_\odot$ of material over the course of its evolution, indicating that the RSG phase for this progenitor cannot be more than $\sim 10^6$ yr, though it is probably less than this. The extent of the region occupied by the RSG wind is set by the pressure of the surrounding interstellar medium, and can range from $\lesssim$1 pc in IIP progenitors to greater than 5 pc in IIb/L

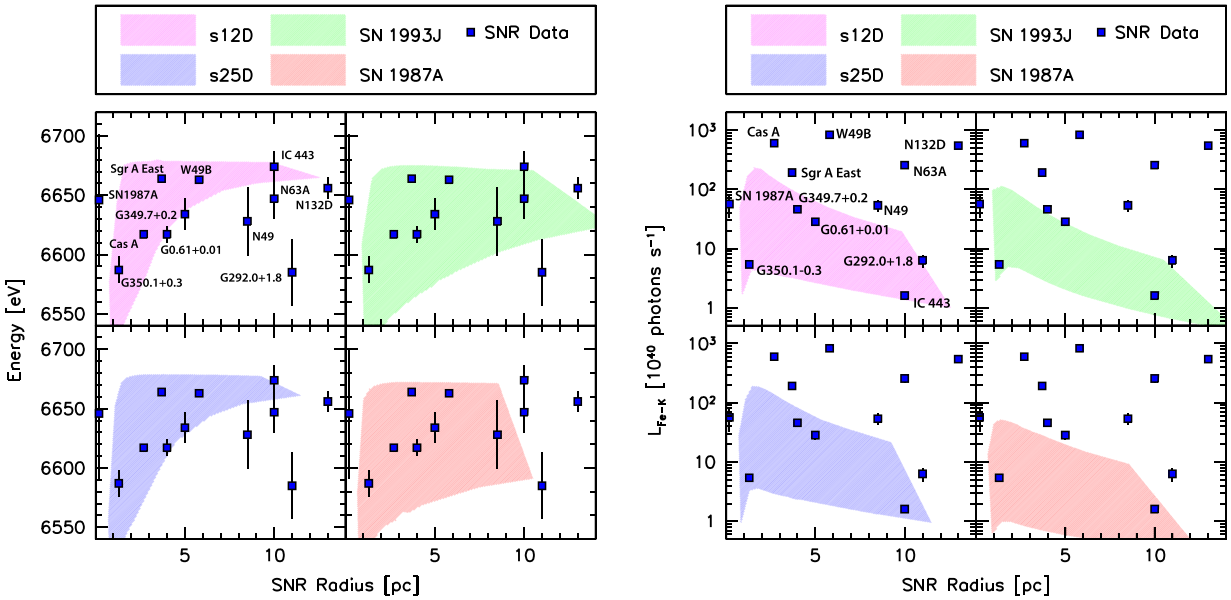

Figure 2. Left: Fe–K line centroid energy as a function of radius for core-collapse supernova remnant measurements and CCSNe models listed in Table 1. Right: Fe–K line luminosity as a function of radius for core-collapse supernova remnant measurements and CCSNe models listed in Table 1.

progenitors (Chevalier 2005). The modeled radii shown in Figure 2 are generally consistent with this, and may suggest that at radii in excess of 10 pc, the wind from an earlier phase of evolution is required—as discussed in Section 2, we applied these models with a broad parameter space, and more detailed modeling for each individual object is necessary.

4.1. Outliers

As seen in Figure 1 (left), while there is generally good agreement between the supernova explosion models and the bulk properties, several CC measurements stand out as having higher than average Fe–K line luminosities: Cas A, N132D, W49B, and N63A. In the case of Cas A, it appears likely that there was bulk overturning of the deepest layers of ejecta during the explosion (Hughes et al. 2000). This resulted in the Fe-rich ejecta being brought to the surface during the explosion. Subsequently, the iron is observed to have been shocked at early times, resulting in a high charge state and luminosity (Hwang & Laming 2003, 2012). The two LMC SNRs N132D and N63A are both thought to be interacting with a large amount of interstellar material in star forming regions, resulting in copious swept up shocked material (Warren et al. 2003; Borkowski et al. 2007).

W49B also displays higher than average Fe–K luminosities, when compared to the other CC SNRs. Lopez et al. (2013) postulated that W49B is the result of a bipolar Type Ib/c SN, based on the morphology and other spectral characteristics. However, the low CSM densities inferred from X-ray and radio observations to be around Ib/c progenitors (e.g., SN 2007gr; Soderberg et al. 2010) appears incongruent with a high Fe–K charge state and line luminosity in the spectrum of W49B. Type Ib/c SNe probably result from WR stars with fast winds and high mechanical luminosities. Compared to red and yellow supergiant progenitors, the 100× faster wind velocities in WR progenitors transport much of the circumstellar material to larger distances, leaving behind a largely low density CSM cavity; though, evidence does exist for more complex environments around some SN Ic, such as in the case of SN 2007bg, which appears to have underwent several differing mass-loss phases prior to the SN (Salas et al. 2013).

Additionally, Ozawa et al. (2009) found evidence for an overionized plasma in W49B, as evidenced by the ratio of H- to He-like lines (see also Lopez et al. 2013; Yamaguchi et al. 2014). Moriya (2012) recently presented a model for SNRs that show overionized plasmas, and suggested that RSG can deposit the mass required for rapid ionization close enough to the progenitor to overionize the shocked material at early times. He noted that the time required to reach ionization equilibrium in a RSG wind is ∼100× faster than in a WR wind, unless collisional ionization equilibrium in the WR wind occurs almost immediately after the explosion (Moriya 2012). However, an emergent class of supernovae typed as Ibn has recently been discovered that displays a strong circumstellar interaction like those found in IIn's as well as no H in the early time optical spectra, like Ib's, such as SN 2006cj (Chugai 2009) and SN 2011w (Smith et al. 2012). The progenitors of these systems include WR and LBVs with zero age main sequence masses $M > 40\ M_{\odot}$, and possibly display eruptive events just prior to the SN Smith (2014). A progenitor such as this may explain both the overionization and high Fe abundance observed in W49B and reconcile these apparently contradictory results with theory. In any event, detailed modeling of a W49B-like progenitor, explosion, and subsequent evolution might be required to explain this odd object.

4.2. Spectral Versus Dynamical Quantities

As seen in Figure 2 (right), our modeled line luminosities fall below the observed values for many remnants. Here we argue that this may be associated with issues related to the very end stages of the progenitor's evolution. While the observed SNR radii appear consistent with the modeled radii, the luminosities differ by more than an order of magnitude. So the question is whether one can increase the luminosity without strongly impacting the radius. For CCSNe, the forward shock radius $R_b \propto \dot{M}^{-1/(n-s)}$ (Chevalier 1982). Thus if one were to increase the mass-loss rate prior to the supernova, we can

estimate the change in blastwave radius as a function of change in $\dot{M}$. First, from Chevalier (1982), the blastwave radius is

$$R_b \propto \left[\frac{Ag^n}{q}\right]^{1/(n-s)} t^{\frac{n-3}{n-s}}, \quad (2)$$

where A is a constant, dependent upon the shape of the ejecta and circumstellar environment, n is the power law index that describes the shape of the ejecta, and s is the power law index that describes the circumstellar environment. In this paper, $n = 9$ and $s = 2$. g^n is a constant, dependent upon the ejecta mass and explosion energy. q is defined as $\dot{M}/4\pi v_w$. If the mass-loss rate is increased by some amount χ prior to the supernova ($q' = \chi q$), such that the blastwave radius is now $R_b' \propto q^{(-1/(n-s))'}$, then the fractional change in the radius, over the extent of time that the blastwave moves through the circumstellar shell is

$$\frac{R_b - R_b'}{R_b} = \frac{q^{-1/(n-s)} - q^{(-1/(n-s))'}}{q^{-1/(n-s)}} \quad (3)$$

$$= 1 - \chi^{-1/(n-s)}. \quad (4)$$

For large changes in the mass-loss rate, this effect can be quite large. For instance, an order of magnitude increase in the mass-loss rate results in a 30% decrease in the blastwave radius. However, we do not expect this increased mass-loss to persist for very long, so the extent of the CSM occupied by the increased density is small, essentially amounting to a thin circumstellar shell. After the blastwave breaks through this shell, it will accelerate into the lower density slow RSG wind.

In contrast, the X-ray luminosity $L_X \sim n_e^2 \Lambda(T) V$, where n_e is the number of free electrons, $\Lambda(T)$ is the cooling function, and V is the emitting volume. Since $n_e \propto \dot{M}$, $L_X \sim \dot{M}^2$. A three-fold increase in the mass-loss rate will result in an approximately order of magnitude increase in L_X, an increase in collisional ionization, and thus an increase in Fe–K line emission. Thus, the problem posed by Figure 2 (right) can be qualitatively addressed by altering the density of the circumstellar environment close to the progenitor. This could be viewed as akin to higher mass-loss just prior to the supernova. We note that this argument may break down for shells that are sufficiently dense to cause significant radiative losses (Crowther 2007; Pan et al. 2013; Smith 2014).

In Figure 2 (left) we plot the modeled and observed Fe–K line centroid versus SNR radii. As shown in Figure 1, the energy centroids for both the model and data are generally greater than 6550 eV. In general, the observed and modeled line centroids as a function of energy are in agreement with one another. However, some SNRs, G292.0+1.8 in particular, do not agree with any of the models. Interestingly, in the line luminosity versus radii plots, G292.0+1.8 also does not agree with the models. This may point to a more complicated circumstellar environment around G292.0+1.8, evidence of which is seen in X-ray observations (Park et al. 2002; Lee et al. 2010). However, in terms of the models, we find that they generally predict Fe–K line centroids in excess of 6550 eV for a broad range of radii. For the high mass-loss rate models, the Fe–K line centroid is approaching collisional ionization equilibrium—increasing the mass-loss rate to affect a change in the luminosity would not alter this conclusion.

5. CONCLUSIONS

We have presented an initial attempt to connect some properties of CCSN, namely the composition and a parameterization of the circumstellar environment, to some observable bulk properties of SNRs. We find that:

1. Using a model for the dynamical and spectral evolution of shocked supernova ejecta and swept up material, we computed Fe–K line centroids and luminosities for a broad range of parameters, including explosion energetics, ejecta mass, and circumstellar environment. We found that they distinctly differ from those same properties computed from models for Type Ia supernovae.
2. We compared our models to measured Fe–K line properties and found general agreement between the models and observations. For those SNRs that do not show good agreement with these simple models we put forth possible reasons for the discrepancy.
3. We discuss the relationship between SNR radius and Fe–K luminosity, and propose that higher mass-loss rates prior to the supernova may be able to reconcile the discrepancy between the modeled and observed luminosities. The required higher mass-loss may arise either through eruptive, episodic events prior to the SNe, such as in SN 2009ip, or increased clumping in the wind during the later stages of evolution. Both of these possibilities would result in a stellar wind profile that differs from the r^{-2} winds considered here.

For CCSNe, the range of ejecta mass, explosion energetics, and circumstellar environment can be large. However, canonical values for supernova parameters can reproduce many observations. Objects such as Cas A and W49B require more detailed models, and any other SNR shown in Figure 1 may be scrutinized in more detail in order to pin down the exact parameter space. In terms of connecting supernovae (and their progenitor) models to SNRs, more detailed studies of young SNRs such as SN 1993J, SN 1996c, and NGC 4449-1 are required in order to bridge the gap between truly young objects and Galactic remnants. Additionally, studies of these objects will allow us to probe the mass-loss history of the progenitor at times $\lesssim 10^5$ yr before the explosion. Future concept X-ray missions with both high imaging and spectral resolution, such as *Smart-X*[9] will foster the detection and study of nearby extragalactic SNRs which can be added to the sample discussed here.

Finally, understanding the mass-loss of supernova progenitors remains a challenge. In this study, we simplified the circumstellar environment to be from a steady wind, though there is substantial evidence that steady line-driven winds may not be prevalent. Understanding clumping in winds as well as episodic mass-loss will be important, as these processes may enhance the phenomena presented here.

We thank R. Fesen and D. Milisavljevic for useful discussions during the preparation of this manuscript. Additionally, we thank the anonymous referee for several useful suggestions that we have incorporated into this paper. D.J.P. acknowledges support for this work through the Smithsonian Institution's Competitive Grants for Science Program. D.J.P. and P.O.S. also acknowledge support from NASA contract

[9] http://smart-x.cfa.harvard.edu

NAS8-03060. S.-H.L. acknowledges support from Grants-in-Aid for Foreign JSPS Fellow (No. 2503018). D.C.E. acknowledges support from NASA grant NNX11AE03G, and S.N. acknowledges support from the Japan Society for the Promotion of Science (Nos. 23340069, 24.02022, 25.03786, and 25610056). A.H. was supported by a Future Fellowship by the Australian Research Council (FT120100363).

REFERENCES

Badenes, C., Bravo, E., Borkowski, K. J., & Domínguez, I. 2003, ApJ, 593, 358
Badenes, C., Borkowski, K. J., Hughes, J. P., Hwang, U., & Bravo, E. 2006, ApJ, 645, 1373
Badenes, C., Hughes, J. P., Bravo, E., & Langer, N. 2007, ApJ, 662, 472
Badenes, C., Hughes, J. P., Cassam-Chenaï, G., & Bravo, E. 2008, ApJ, 680, 1149
Bauer, F. E., Dwarkadas, V. V., Brandt, W. N., et al. 2008, ApJ, 688, 1210
Blondin, J. M., & Lufkin, E. A. 1993, ApJS, 88, 589
Borkowski, K. J., Hendrick, S. P., & Reynolds, S. P. 2007, ApJL, 671, L45
Chevalier, R. A. 1982, ApJ, 258, 790
Chevalier, R. A., & Emmering, R. T. 1989, ApJL, 342, L75
Chevalier, R. A. 2005, ApJ, 619, 839
Chiotellis, A., Schure, K. M., & Vink, J. 2012, A&A, 537, A139
Chugai, N. N. 2009, MNRAS, 400, 866
Crowther, P. A. 2007, ARA&A, 45, 177
Dwarkadas, V. V., & Chevalier, R. A. 1998, ApJ, 497, 807
Dwarkadas, V. V., & Gruszko, J. 2012, MNRAS, 419, 1515
Dwarkadas, V. V. 2007, ApJ, 667, 226
Dwarkadas, V. V. 2011, MNRAS, 412, 1639
Ellison, D. C., Patnaude, D. J., Slane, P., Blasi, P., & Gabici, S. 2007, ApJ, 661, 879
Ellison, D. C., Patnaude, D. J., Slane, P., & Raymond, J. 2010, ApJ, 712, 287
Ellison, D. C., Slane, P., Patnaude, D. J., & Bykov, A. M. 2012, ApJ, 744, 39
Fesen, R. A., & Matonick, D. M. 1993, ApJ, 407, 110
Filippenko, A. V. 1997, ARA&A, 35, 309
Fransson, C., Chevalier, R. A., Filippenko, A. V., et al. 2002, ApJ, 572, 350
Fransson, C., Lundqvist, P., & Chevalier, R. A. 1996, ApJ, 461, 993
Gal-Yam, A., Leonard, D. C., Fox, D. B., et al. 2007, ApJ, 656, 372
Hashimoto, M., Nomoto, K., & Shigeyama, T. 1989, A&A, 210, L5
Heger, A., & Woosley, S. E. 2010, ApJ, 724, 341
Hughes, J. P., Hayashi, I., Helfand, D., et al. 1995, ApJL, 444, L81
Hughes, J. P., Rakowski, C. E., Burrows, D. N., & Slane, P. O. 2000, ApJL, 528, L109
Hwang, U., & Laming, J. M. 2003, ApJ, 597, 362
Hwang, U., & Laming, J. M. 2012, ApJ, 746, 130
Joggerst, C. C., Woosley, S. E., & Heger, A. 2009, ApJ, 693, 1780
Koo, B.-C., & McKee, C. F. 1992, ApJ, 388, 93
Krause, O., Birkmann, S. M., Usuda, T., et al. 2008, Sci, 320, 1195
Lee, J.-J., Park, S., Hughes, J. P., et al. 2010, ApJ, 711, 861
Lee, S.-H., Patnaude, D. J., Ellison, D. C., Nagataki, S., & Slane, P. O. 2014, ApJ, 791, 97
Lodders, K., Palme, H., & Gail, H.-P. 2009, LanB, 4, 44
Lopez, L. A., Ramirez-Ruiz, E., Castro, D., & Pearson, S. 2013, ApJ, 764, 50
Lopez, L. A., Pearson, S., Ramirez-Ruiz, E., et al. 2013, ApJ, 777, 145
Milisavljevic, D., Fesen, R. A., Chevalier, R. A., et al. 2012, ApJ, 751, 25
Moriya, T. J. 2012, ApJL, 750, L13
Nozawa, T., Kozasa, T., Tominaga, N., et al. 2010, ApJ, 713, 356
Ozawa, M., Koyama, K., Yamaguchi, H., Masai, K., & Tamagawa, T. 2009, ApJL, 706, L71
Pan, T., Patnaude, D., & Loeb, A. 2013, MNRAS, 433, 838
Park, S., Roming, P. W. A., Hughes, J. P., et al. 2002, ApJL, 564, L39
Patnaude, D. J., Ellison, D. C., & Slane, P. 2009, ApJ, 696, 1956
Patnaude, D. J., Slane, P., Raymond, J. C., & Ellison, D. C. 2010, ApJ, 725, 1476
Patnaude, D. J., Badenes, C., Park, S., & Laming, J. M. 2012, ApJ, 756, 6
Rauscher, T., Heger, A., Hoffman, R. D., & Woosley, S. E. 2002, ApJ, 576, 323
Rest, A., Welch, D. L., Suntzeff, N. B., et al. 2008, ApJL, 681, L81
Saio, H., Nomoto, K., & Kato, M. 1988, Natur, 334, 508
Salas, P., Bauer, F. E., Stockdale, C., & Prieto, J. L. 2013, MNRAS, 428, 1207
Sana, H., de Mink, S. E., de Koter, A., et al. 2012, Sci, 337, 444
Shigeyama, T., & Nomoto, K. 1990, ApJ, 360, 242
Shigeyama, T., Suzuki, T., Kumagai, S., et al. 1994, ApJ, 420, 341
Smartt, S. J., Gilmore, G. F., Tout, C. A., & Hodgkin, S. T. 2002, ApJ, 565, 1089
Smartt, S. J. 2009, ARA&A, 47, 63
Smith, N. 2014, ARA&A, 52, 487
Smith, N., Chornock, R., Li, W., et al. 2008, ApJ, 686, 467
Smith, N., Mauerhan, J. C., Silverman, J. M., et al. 2012, MNRAS, 426, 1905
Soderberg, A. M., Brunthaler, A., Nakar, E., Chevalier, R. A., & Bietenholz, M. F. 2010, ApJ, 725, 922
Truelove, J. K., & McKee, C. F. 1999, ApJS, 120, 299
Warren, J. S., Hughes, J. P., & Slane, P. O. 2003, ApJ, 583, 260
Weaver, T. A., Zimmerman, G. B., & Woosley, S. E. 1978, ApJ, 225, 1021
Woosley, S. E., & Heger, A. 2007, PhR, 442, 269
Woosley, S. E., Heger, A., & Weaver, T. A. 2002, RvMP, 74, 1015
Yamaguchi, H., Badenes, C., Petre, R., et al. 2014, ApJL, 785, L27